Event-Triggered Optimal Power Dispatch

M.D. Lemmon, University of Notre Dame

I. Introduction

Microgrids [14] [11] [9] are power generation/distribution systems in which users and generators are in close proximity. This results in relatively low voltage grids (few hundred kVA). Generation is often done using renewable generation sources such as photovoltaic cells or wind turbines. Power generation can also be accomplished through small microturbines and gas/diesel generators. Storage devices such as battery banks represent another important power source for microgrids. These units can be used in places such as office buildings, parks, homes and battle fields as distributed power sources. They are modular in the sense that, if needed, new unit can be added to the network in an easy way. All the microgrids in the network can work in a cooperative way to meet the overal load demand in the network.

Active/reactive power dispatch problems have been the research subject of power system community since in the early 1960's. The problem is usually formulated as an optimal power flow (OPF) problem. The OPF problem [16] [10] is an important class of problems in the power industry. The problem is to determine generator power set points so that the overall cost of power generation is minimized, while respecting limits on the generator's capacity and transmission power flow constraints.

Various centralized or distributed optimization algorithms have been proposed to solve the OPF problem, including network flow approach [6], interior point method [16] [10], multi-area decomposition [8] [4] [12], etc. These algorithms usually made the assumptions that communication between subsystems was not expensive and reliable. This assumption, however, is not always realistic since one of the first things to go down during power disruptions is the communication network. One way around this problem is to make use of low power ad hoc wireless communication networks that operate independently of the main power grid.

Ad hoc wireless sensor networks have recently been used in the reliable operation and control of various civil infrastructure systems [17][15]. The nodes in these networks are usually powered by batteries or solar arrays, so they would unaffected by fluctuations in the main power grid. These networks, however, have severe throughput limitations that make it impractical to send a large amount of information across the network. Moreover, it may be impractical to send periodically sampled data across the network as the nodes in these networks have limited power due to their reliance on batteries. As a result of these considerations, ad hoc communication networks can provide a power grid's communication infrastructure only if we can greatly limit the amount of information that needs to be transmitted across the network. One way of doing this is to adopt an *event-triggered* approach to information transmission.

Event-triggered systems are systems in which sensors are sampled in a *sporadic* non-periodic manner. Event-triggering has an agent transmit information to its neighbors when some measure of the "novelty" in that information exceeds a specified threshold. In this way, the communication network is only used when there is an immediate need. Early examples of event-triggering were used in relay control systems[20] and more recent work has looked at event-triggered PID controllers [1]. Much of the early work in event-triggered control assumed event-triggers in which the triggering thresholds were constant. Recently it was shown that state-dependent event triggers could be used to enforce stability concepts such as input-to-state stability [19] or $\mathscr{L}_2$ stability [22] in both embedded control systems and networked control systems [23]. There has been ample experimental evidence [2], [18] to suggest that event-triggering can greatly reduce communication bandwidth while preserving overall system performance. Much more recently, our own work [21] has shown that event-triggering can greatly reduce (by several orders of magnitude) the message passing required in the solution of network utility maximization problems. Event-triggering therefore provides a useful approach for reducing an application's use of the communication network.

II. Power Flow Problem

his section reviews the DC flow model [7], which is widely used to characterize a power system's behavior around the normal steady state operation. The power system can be modeled as a directed graph. Consider a connected directed graph $G = (\mathscr{V}, \mathscr{E}, A)$ as an abstraction of an

electrical power network. The system consists of N buses. For simplicity of discussion, we assume that each bus has a local generator and a local load connected to it in our model. More general scenarios where a certain bus does not have a local generator or has multiple local loads can be treated similarly without much difficulty. $\mathscr{V} = \{v_1, ..., v_N\}$ is the set of nodes, and each node represents a bus (with a local generator and load). $\mathscr{E} \subseteq \mathscr{V} \times \mathscr{V}$ is the set of directed edges, which corresponds to the power transmission lines. Suppose the network has $M = |\mathscr{E}|$ edges, and they are ordered $1, 2, ..., M$. An edge from node i to node j is denoted as $e_{ij} = (v_i, v_j)$. $z_{ij} = r_{ij} + jx_{ij}$ is the impedance of the transmission line corresponding to edge e_{ij}. Since r_{ij} is often negligible compared to x_{ij}, we can assume $r_{ij} = 0$ in our DC flow model. Suppose the incidence matrix [5] of graph G is I, and define a diagonal matrix $D \in \mathbb{R}^{M \times M}$, whose diagonal entries are the reactances x of M transmission lines. Then the weighted incidence matrix $A \in \mathbb{R}^{M \times N}$ is defined as $A = DI$. The set of neighbors of node i is defined as $\mathscr{N}(i) = \{v_j \in \mathscr{V} | (v_i, v_j) \in \mathscr{E}\}$, and node i has $|\mathscr{N}(i)|$ neighbors. The set of transmission lines that leave bus i is defined as $\mathscr{L}(i) = \{e_{ij} \in \mathscr{E} | j \in \mathscr{N}(i)\}$.

Let $S_{ij} = P_{ij} + jQ_{ij}$ denote the complex power flow from node i to node j, and u_i denote the generator voltage at node i. Use the following magnitude-phase representation,

$$u_i = |u_i| e^{j\theta_i}, \quad u_j = |u_j| e^{j\theta_j} \tag{1}$$

and remember the line impedance may be approximated as $z_{ij} = jx_{ij}$. Under normal operating conditions, the bus voltages are about equal ($|u_i| \approx |u_j|$). In a similar manner, the bus phases are about equal so that the phase difference, $\theta_i - \theta_j$, is typically small. In this case, there is reasonably good decoupling between the control of active power flow P_{ij} and reactive power flow Q_{ij}. The active power flow is mainly dependent on $\theta_i - \theta_j$, and the reactive power flow is mainly dependent on $|u_i| - |u_j|$.

The DC flow model we are using further assumes that only the voltage phases θ_i, θ_j vary, and that variation is small. Voltage magnitudes $|u_i|$, $|u_j|$ are assumed to be constant ($|u_i| = |u_j| = 1$ here). In this case, the reactive power flow Q_{ij} is negligible, and we are only considering the active power flow P_{ij}. With the assumptions and simplifications above, the power flow from node i to node j is given by

$$P_{ij} = \frac{1}{x_{ij}} (\theta_i - \theta_j) \tag{2}$$

The total power flowing into bus i, P_i, must equal the power generated by generator i minus

the power absorbed by the local load at the bus. P_i, therefore, must equal the the sum of the power flowing away from bus i on all transmission lines. This means

$$P_i = \sum_{j \in \mathcal{N}(i)} P_{ij} = \sum_{j \in \mathcal{N}(i)} \frac{1}{x_{ij}} (\theta_i - \theta_j) \tag{3}$$

which can be expressed in a matrix form

$$P = B\theta \tag{4}$$

where $P = [P_1, ..., P_N]^T$, $\theta = [\theta_1, ..., \theta_N]^T$, and B is defined as

$$B_{ij} = \begin{cases} \sum_{j \in \mathcal{N}(i)} \frac{1}{x_{ij}}, & \text{if} \quad i = j, \\ -\frac{1}{x_{ij}}, & \text{if} \quad e_{ij} \in E, \\ 0, & \text{if} \quad e_{ij} \notin E \end{cases} \tag{5}$$

B is a singular matrix, which can be thought as a weighted Laplacian matrix [5] of the graph. The weight here is $1/x_{ij}$ for edge e_{ij}.

Based on our DC flow model in equation 2, we can formulate the **General OPF problem** as follows :

$$\text{minimize} \quad C(P_G) = \textstyle\sum_{i=1}^{N} C_i(P_{G_i}) \tag{6}$$

$$\text{w.r.t} \qquad P_G \tag{7}$$

$$\text{subject to:} \qquad B\theta = P_G - P_L \tag{8}$$

$$\underline{P_G} \leq P_G \leq \overline{P_G} \tag{9}$$

$$\underline{P} \leq A\theta \leq \overline{P} \tag{10}$$

Here $P_G = [P_{G_1}, ..., P_{G_N}]^T$ is the vector of generated active powers for all generators, and $P_L = [P_{L_1}, ..., P_{L_N}]^T$ is the vector of total local loads for all buses. A and B are sparse matrices and have been defined previously. $\underline{P_G} = \{\underline{P_{G_1}}, \cdots, \underline{P_{G_N}}\}$ and $\overline{P_G} = \{\overline{P_{G_1}}, \cdots, \overline{P_{G_N}}\}$ represent the lower and upper limits of the generators' power generating constraints. $\underline{P} = \{\underline{P_1}, \cdots, \underline{P_M}\}$ and $\overline{P} = \{\overline{P_1}, \cdots, \overline{P_M}\}$ represent the lower and upper limits of the power flows on the transmission lines. Here P_L, $\underline{P_G}$, $\overline{P_G}$, $\underline{P}$ and $\overline{P}$ are known constants in the problem formulation, and A and B are known constant matrices. The objective function in equation 6 represents the total generation

cost of all the generators, and generator i's cost of generating P_{G_i} unit of active power is usually in the form of

$$C_i(P_{G_i}) = a_i + b_i P_{G_i} + c_i P_{G_i}^2 \tag{11}$$

where a_i, b_i and c_i are constant coefficients. The constraint in equation 8 is the power flow balance equation. Constraints in equation 9 and 10 represent the generation limits of the generators, and power flow limits on the transmission lines, respectively. The General OPF problem seeks to find the optimal generated active power P_G such that the total generation cost is minimized, subject to the power flow equation and physical constraints of the generation and transmission systems.

To apply the idea of event-triggered optimization, we need to reformulate the previous General OPF problem to fit into the NUM problem formulation and adopt a similar approach we have used in [21]. This is done by recognizing that the constraint in equation 9 is a power balance relation that is always maintained within the system. We can therefore remove P_G as a control variable to obtain the following **revised OPF problem**.

$$\text{minimize} \quad C(P_G) = \sum_{i=1}^{N} C_i((B\theta)_i + P_{L_i}) \tag{12}$$

$$\text{w.r.t} \qquad \theta \tag{13}$$

$$\text{subject to:} \qquad \underline{P_G} - P_L \leq B\theta \leq \overline{P_G} - P_L \tag{14}$$

$$\underline{P} \leq A\theta \leq \overline{P} \tag{15}$$

where $(B\theta)_i$ is the ith element of $B\theta$. Note that the new optimization problem is solved with respect to the phase angle θ instead of P_G. The revised OPF problem also has the same solution as the General OPF problem. We will solve the revised OPF problem later in section **??** using an event-triggered distributed algorithm.

III. The CERTS Microgrid model

This section briefly describes the CERTS microgrid model and the microsource controller developed by the University of Wisconsin, Madison (UWM). A detailed account of the microsource controllers can be found in [13]. Since we are using the CERTS microgrid model in our MATLAB/SimPower simulation, the basic operation of the model and the controller is described below.

The inverter-based microsource consists of a D.C. source whose outputs are transformed into an A.C. voltage through an inverter. The actions of the inverter are guided by a controller that uses sensed feeder currents and voltages to determine how best to control the operation of the inverter. Figure 1 shows that the output of the inverter is passed through a low pass filter to remove switching transients to produce a three phase 480V voltage. A transformer then steps this down to 208 V (120 volts rms).

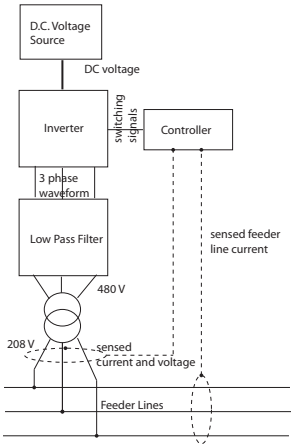

Fig. 1. inverter-based microsource

The UWM microsource controller is shown in figure 2. The inputs are measurements of inverter current, load voltage and line current. The controller also takes as reference inputs the requested voltage level E_{req}, the requested power set point P_{req}, and the desired frequency f_{req} (usually 60 Hz). The controller takes the measured inputs and computes the instantaneous reactive power, Q, the voltage magnitude, E, and the real power P. These computed values are low pass filtered. The reactive power, Q, and the requested voltage E_{req} are input to the Q vs E droop controller to determine the desired voltage level. This is compared against the measured voltage level and the output V is then given to the gate pulse generator. Another channel in the controller uses the measured real power and implements another droop control that balances the system's frequency against the requested power level, P_{req}. The output of the P vs frequency droop controller is used to adjust the phase angle, δ_V, which is also fed into the gate pulse generator. The output of the gate pulse generator goes directly into the inverter.

The action of this controller is, essentially, to mimic the droop controls seen in traditional

synchronous generators. This means that if a load begins drawing a great deal of real power, then the line frequency will "droop" as an indicator of the extra stress on the system. The controller automatically tries to restore that frequency to its desired levels. But it will be unable to restore the droop if the power being pulled if the power drawn by the load exceeds the generator's capacity. This drop in frequency can be sensed at the load and may be used to help decide if the load should disconnect from the microgrid. A similar scenario occurs if the load begins drawing too much reactive power. In this case, there will be a droop in the voltage that can again be used by the load to determine if it should disconnect from the grid. These droop controllers are well understood and they can be easily interfaced to price-based power control methods through the requested power and voltage set points shown in figure 2. The event-triggered control inputs developed in this paper will interface to this controller through the requested power input.

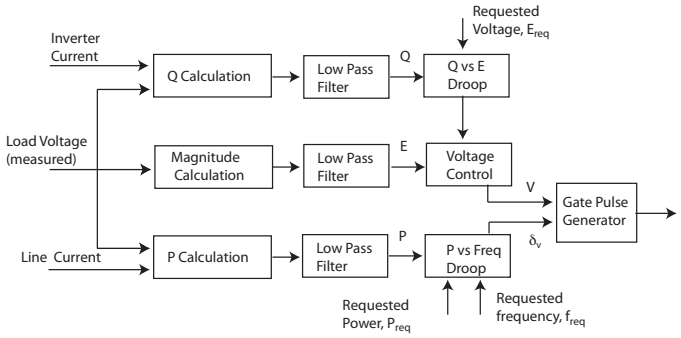

Fig. 2. UWM microsource controller

IV. Event-triggered optimization for OPF

The event-triggered algorithm can be easily integrated into the CERTS microgrid model by dynamically adjusting the power set point of each generator.

The revised OPF problem is a constrained problem, which can be converted into a sequence of unconstrained problems by adding to the cost function a penalty term that prescribes a high cost to infeasible points.

Take the $A\theta \leq \overline{P}$ constraint for example, we can introduce a slack variable $s \in \mathbb{R}^M$ and replace the inequalities $\overline{P_j} - a_j^T \theta \geq 0$, $\forall j \in \mathscr{E}$ by

$$a_j^T \theta - \overline{P_j} + s_j = 0, \quad s_j \geq 0, \quad \forall j \in \mathscr{E} \tag{16}$$

Here the vector $a_j^T = \left[A_{j1}, \cdots, A_{jN}\right]$ is the jth row of matrix A.

Define

$$\overline{\psi_j}(\theta; w^{\mathscr{E}}) = \min_{s_j \geq 0} \frac{1}{2w_j^{\mathscr{E}}}(a_j^T\theta - \overline{P_j} + s_j)^2 \tag{17}$$

where a penalty parameter $w_j^{\mathscr{E}}$ is associated with each transmission line j and $w^{\mathscr{E}} = \left[w_1^{\mathscr{E}}, \cdots, w_M^{\mathscr{E}}\right]$ is the vector of transmission line penalty parameters.

It is easy to show that

$$\overline{\psi_j}(\theta; w^{\mathscr{E}}) = \begin{cases} 0, & \text{if} \quad \overline{P_j} - a_j^T\theta \geq 0 \\ \frac{1}{2w_j^{\mathscr{E}}}(a_j^T\theta - \overline{P_j})^2, & \text{otherwise} \end{cases}$$

Similarly we can define

$$\underline{\psi_j}(\theta; w^{\mathscr{E}}) = \begin{cases} 0, & \text{if} \quad \underline{P_j} - a_j^T\theta \leq 0 \\ \frac{1}{2w_j^{\mathscr{E}}}(a_j^T\theta - \underline{P_j})^2, & \text{otherwise} \end{cases}$$

which corresponds to the inequality constraint $\underline{P_j} - a_j^T\theta \leq 0$, $\forall j \in \mathscr{E}$.

Define $b_k^T = [B_{k1}, \cdots, B_{kN}]$ as the kth row of matrix B and let $w^{\mathscr{V}} = \left[w_1^{\mathscr{V}}, \cdots, w_N^{\mathscr{V}}\right]$ denote the vector of generator penalty parameters. This gives us

$$\overline{\chi_k}(\theta; w^{\mathscr{V}}) = \begin{cases} 0, & \text{if} \quad \overline{P_{G_k}} - P_{L_k} - b_k^T\theta \geq 0 \\ \frac{1}{2w_k^{\mathscr{V}}}(b_k^T\theta - \overline{P_{G_k}} + P_{L_k})^2, & \text{otherwise} \end{cases}$$

for constraint $b_k^T\theta - \overline{P_{G_k}} + P_{L_k} \leq 0$, $\forall k \in \mathscr{V}$ and

$$\underline{\chi_k}(\theta; w^{\mathscr{V}}) = \begin{cases} 0, & \text{if} \quad \underline{P_{G_k}} - P_{L_k} - b_k^T\theta \leq 0 \\ \frac{1}{2w_k^{\mathscr{V}}}(b_k^T\theta - \underline{P_{G_k}} + P_{L_k})^2, & \text{otherwise} \end{cases}$$

for constraint $b_k^T\theta - \underline{P_{G_k}} + P_{L_k} \geq 0$, $\forall k \in \mathscr{V}$.

Let us define the *the augmented cost* as

$$\begin{aligned} L(\theta; w^{\mathscr{E}}, w^{\mathscr{V}}) = &\sum_{i \in \mathscr{V}} C_i((B\theta)_i + P_{L_i}) + \sum_{j \in \mathscr{E}} \overline{\psi_j}(\theta; w^{\mathscr{E}}) + \\ &\sum_{j \in \mathscr{E}} \underline{\psi_j}(\theta; w^{\mathscr{E}}) + \sum_{i \in \mathscr{V}} \overline{\chi_i}(\theta; w^{\mathscr{V}}) + \sum_{i \in \mathscr{V}} \underline{\chi_i}(\theta; w^{\mathscr{V}}) \end{aligned} \tag{18}$$

$L(\theta; w^{\mathscr{E}}, w^{\mathscr{V}})$ is a continuous function of θ for fixed $w^{\mathscr{E}}$ and $w^{\mathscr{V}}$. Let $\theta^*[k]$ denote the approximate minimizer of $L(\theta; w^{\mathscr{E}}[k], w^{\mathscr{V}}[k])$. It was shown in [3] that by approximately minimizing

$L(\theta; w^{\mathscr{E}}, w^{\mathscr{V}})$ for sequences of $\{w^{\mathscr{E}}[k]\}_{k=0}^{\infty}$ and $\{w^{\mathscr{V}}[k]\}_{k=0}^{\infty}$, the sequence of approximate minimizers $\{\theta^*[k]\}_{k=0}^{\infty}$ converges to the optimal point of the OPF problem. We only require that $\{w_j^{\mathscr{E}}[k]\}_{k=0}^{\infty}$ and $\{w_i^{\mathscr{V}}[k]\}_{k=0}^{\infty}$, $\forall j \in \mathscr{E}$, $\forall i \in \mathscr{V}$ are sequences of transmission line/generator penalty parameters that are monotone decreasing to zero.

Instead of minimizing $L(\theta; w^{\mathscr{E}}, w^{\mathscr{V}})$ for sequences of penalty parameters, we are only considering the problem of minimizing $L(\theta; w^{\mathscr{E}}, w^{\mathscr{V}})$ for fixed $w^{\mathscr{E}}$ and $w^{\mathscr{V}}$ in this paper. If $w_j^{\mathscr{E}}$ and $w_i^{\mathscr{V}}$ are sufficiently small, the minimizer of $L(\theta; w^{\mathscr{E}}, w^{\mathscr{V}})$ will be a good approximation to the solution of the original OPF problem. We should note that in our earlier work in [21], we gave an event-triggered algorithm that converges to the exact minimizer of the NUM problem. Interested reader can refer to that paper to see how we can decrease the penalty parameters in a distributed way to accomplish that.

We can search for the minimizer of $L(\theta; w^{\mathscr{E}}, w^{\mathscr{V}})$ using a gradient descent algorithm where

$$\theta_i(t) \;=\; -\int_0^t \nabla_{\theta_i} L(\theta(\tau); w^{\mathscr{E}}, w^{\mathscr{V}}) d\tau$$

for each generator $i \in \mathscr{V}$. The derivative of $L(\theta; w^{\mathscr{E}}, w^{\mathscr{V}})$ with respect to θ_i can be shown to be

$$\begin{aligned}
&\nabla_{\theta_i} L(\theta; w^{\mathscr{E}}, w^{\mathscr{V}}) \\
=\;& \sum_{j \in \mathscr{L}(i)} \max\{0, \frac{1}{w_j^{\mathscr{E}}}(a_j^T\theta - \overline{P_j})\} A_{ji} \\
+\;& \sum_{j \in \mathscr{L}(i)} \min\{0, \frac{1}{w_j^{\mathscr{E}}}(a_j^T\theta - \underline{P_j})\} A_{ji} \\
+\;& \sum_{k \in \mathscr{N}(i)+i} \max\{0, \frac{1}{w_k^{\mathscr{V}}}(b_k^T\theta - \overline{P_{G_k}} + P_{L_k})\} B_{ki} \\
+\;& \sum_{k \in \mathscr{N}(i)+i} \min\{0, \frac{1}{w_k^{\mathscr{V}}}(b_k^T\theta - \underline{P_{G_k}} + P_{L_k})\} B_{ki} \\
+\;& \sum_{k \in \mathscr{N}(i)+i} \nabla C_k(b_k^T\theta + P_{L_k}) B_{ki}
\end{aligned}$$

For each transmission line, let us define

$$\begin{aligned}
\mu_j(t) \;&=\; \max\{0, \frac{1}{w_j^{\mathscr{E}}}(a_j^T\theta(t) - \overline{P_j})\} \\
&+\; \min\{0, \frac{1}{w_j^{\mathscr{E}}}(a_j^T\theta(t) - \underline{P_j})\}
\end{aligned} \tag{19}$$

Here $a_j^T\theta(t)$ is simply the power flow on transmission line $j \in \mathscr{E}$ at time t. $w_j^{\mathscr{E}} > 0$ is a constant penalty coefficients that penalizes the violation of the transmission line flow limits. It is easy to see that $\mu_j(t)$ is nonzero if and only if the flow on the jth transmission line exceeds the line flow limits. $\mu_j(t)$ summarizes the information of the jth transmission line at time t and can be viewed as its state.

Similarly for each generator $k \in \mathscr{V}$ we define

$$\begin{aligned}\varphi_k(t) &= \nabla C_k(b_k^T\theta(t) + P_{L_k}) \\ &+ \max\{0, \frac{1}{w_k^{\mathscr{V}}}(b_k^T\theta(t) + P_{L_k} - \overline{P_{G_k}})\} \\ &+ \min\{0, \frac{1}{w_k^{\mathscr{V}}}(b_k^T\theta(t) + P_{L_k} - \underline{P_{G_k}})\}\end{aligned}$$

Here $w_k^{\mathscr{V}}$ is a constant penalty coefficient that penalizes the violation of the generating limits for generator $k \in \mathscr{V}$. Recall the power balance equation in 8 and we can thus rewrite $\varphi_k(t)$ as

$$\begin{aligned}\varphi_k(t) &= \nabla C_k(P_{G_k}(t)) + \max\{0, \frac{1}{w_k^{\mathscr{V}}}(P_{G_k}(t) - \overline{P_{G_k}})\} \\ &+ \min\{0, \frac{1}{w_k^{\mathscr{V}}}(P_{G_k}(t) - \underline{P_{G_k}})\}\end{aligned}$$

It is then easy to see that $\varphi_k(t)$ is determined by the gradient of the current generation cost of the kth generator, and whether the kth generator's generation limit is satisfied. In other words, $\varphi_k(t)$ summarizes the information of the kth generator at time t and can be viewed as its state.

We can now rewrite the derivative of $L(\theta; w^{\mathscr{E}}, w^{\mathscr{V}})$ with respect to θ_i as

$$\nabla_{\theta_i} L(\theta; w^{\mathscr{E}}, w^{\mathscr{V}}) = \sum_{j \in \mathscr{L}(i)} \mu_j A_{ji} + \sum_{k \in \mathscr{N}(i)+i} \varphi_k B_{ki} \tag{20}$$

and the gradient descent algorithm takes the form

$$\theta_i(t) = -\int_0^t \left[\sum_{j \in \mathscr{L}(i)} \mu_j(\tau) A_{ji} + \sum_{k \in \mathscr{N}(i)+i} \varphi_k(\tau) B_{ki} \right] d\tau \tag{21}$$

Note that in equation 21, generator i can compute its phase angle only based on the state φ_i from itself and its neighboring generators, as well as the state μ_j from its outgoing transmission lines. The update of θ_i can be done in a distributed manner.

However, in the above equation, this neighboring generator's state information is available to generator i in a continuous manner, which would require continuous communications between

neighboring generators. This is highly undesirable. An *event-triggered* version of equation 21 assumes that generator i accesses a *sampled* version of its neighboring generator's state. In particular, let's associate a sequence of *sampling* instants, $\{T_i[\ell]\}_{\ell=0}^{\infty}$ with the ith generator. The time $T_i[\ell]$ denotes the instant when the ith generator samples its state φ_i for the ℓth time and transmits that state to neighboring generators $k \in \mathscr{N}(i)$. We can see that at any time $t \in \Re$, the sampled generator state is a piecewise constant function of time in which

$$\hat{\varphi}_i(t) = \varphi_i(T_i[\ell]) \tag{22}$$

for all $\ell = 0, \cdots, \infty$ and any $t \in [T_i[\ell], T_i[\ell+1])$. In this regard, the "event-triggered" version of equation 21 takes the form

$$\begin{aligned} \theta_i(t) &= -\int_0^t \Bigg[\sum_{j \in \mathscr{L}(i)} \mu_j(\tau) A_{ji} \\ &\quad + \sum_{k \in \mathscr{N}(i)} \hat{\varphi}_k(\tau) B_{ki} + \varphi_i(\tau) B_{ii} \Bigg] d\tau \end{aligned} \tag{23}$$

for all ℓ and any $t \in [T_i[\ell], T_i[\ell+1])$.

The sequence $\{T_i[\ell]\}_{\ell=0}^{\infty}$ represents time instants when generator i transmits its "state" to its neighboring generators. Here we assume that there is no transmission delay in each $\hat{\varphi}_i(t)$ broadcast.

Next we will state the main theorem of this subsection, which states the condition under which each generator should sample and broadcast its state.

Theorem: Consider the Lagrangian in equation 18 where the functions C_i are differentiable, strictly increasing, and convex. Assume fixed generator and transmission line penalty parameters $w^{\mathscr{E}} > 0$, $w^{\mathscr{V}} > 0$. $\forall i \in \mathscr{V}$, define

$$z_i(t) = \sum_{j \in \mathscr{L}(i)} \mu_j(\tau) A_{ji} + \sum_{k \in \mathscr{N}(i)} \hat{\varphi}_k(\tau) B_{ki} + \varphi_i(\tau) B_{ii}$$

and

$$\rho_i = 1 / \sqrt{\sum_{k=1}^{N} |\mathscr{N}(k)| B_{ik}^2} \tag{24}$$

Consider the sequences $\{T_i[\ell]\}_{\ell=0}^{\infty}$ for each $i \in \mathscr{V}$. For each generator $i \in \mathscr{V}$, let its phase angle, $\theta_i(t)$, satisfy equation 23 with sampled neighboring state given by equation 22. Assume

that for all $i \in \mathscr{V}$ and all $\ell = 0, \cdots, \infty$, that

$$|\varphi_i(t) - \hat{\varphi}_i(t)| \leq \rho_i |z_i(t)| \tag{25}$$

for $t \in [T_i[\ell], T_i[\ell+1])$. Then the phase angle $\theta(t)$ asymptotically converge to the unique minimizer of $L(\theta; w^{\mathscr{E}}, w^{\mathscr{V}})$. ■

Proof: For convenience, we do not explicitly include the time dependence in the proof.

For all $t \geq 0$ we have

$$\begin{aligned}
& -\dot{L}(\theta; w^{\mathscr{E}}, w^{\mathscr{V}}) \\
= & -\sum_{i=1}^{N} \frac{\partial L}{\partial \theta_i} \frac{d\theta_i}{dt} \\
= & \sum_{i=1}^{N} z_i \left[\sum_{j \in \mathscr{L}(i)} \mu_j A_{ji} + \sum_{k \in \mathscr{N}(i)} \varphi_k B_{ki} + \varphi_i B_{ii} \right] \\
\geq & \frac{1}{2} \sum_{i=1}^{N} \left\{ z_i^2 - \left[\sum_{k \in \mathscr{N}(i)} (\varphi_k - \hat{\varphi}_k) B_{ki} \right]^2 \right\} \\
\geq & \frac{1}{2} \sum_{i=1}^{N} z_i^2 - \frac{1}{2} \sum_{i=1}^{N} |\mathscr{N}(i)| \sum_{k \in \mathscr{N}(i)} [(\varphi_k - \hat{\varphi}_k) B_{ki}]^2 \\
= & \frac{1}{2} \sum_{i=1}^{N} z_i^2 - \frac{1}{2} \sum_{i=1}^{N} |\mathscr{N}(i)| \sum_{k=1}^{N} [(\varphi_k - \hat{\varphi}_k) B_{ki}]^2 \\
= & \frac{1}{2} \sum_{i=1}^{N} z_i^2 - \frac{1}{2} \sum_{k=1}^{N} (\varphi_k - \hat{\varphi}_k)^2 \sum_{i=1}^{N} |\mathscr{N}(i)| B_{ki}^2 \\
= & \frac{1}{2} \sum_{i=1}^{N} z_i^2 - \frac{1}{2} \sum_{i=1}^{N} \left(\sum_{k=1}^{N} |\mathscr{N}(k)| B_{ik}^2 \right) (\varphi_i - \hat{\varphi}_i)^2
\end{aligned}$$

which immediately suggests that if the sequences of sampling instants $\{T_i[\ell]\}_{\ell=0}^{\infty}$ satisfy the inequality in equation 25 for all $\ell = 0, 1, 2, ..., \infty$, and any $i \in \mathscr{V}$, then $\dot{L}(\theta; w^{\mathscr{E}}, w^{\mathscr{V}}) \leq 0$ is guaranteed for all t.

By using the properties of C_i and $\overline{\psi_j}(\theta; w^{\mathscr{E}})$, $\underline{\psi_j}(\theta; w^{\mathscr{E}})$, $\overline{\chi_k}(\theta; w^{\mathscr{V}})$, $\underline{\chi_k}(\theta; w^{\mathscr{V}})$, it is easy to show that for any fixed $w^{\mathscr{E}}$ and $w^{\mathscr{V}}$, $L(\theta; w^{\mathscr{E}}, w^{\mathscr{V}})$ is strictly convex in θ. It thus has a unique minimizer. Suppose $\theta^*(w^{\mathscr{E}}, w^{\mathscr{V}})$ is this minimizer, and the corresponding Lagrangian is $L(\theta^*; w^{\mathscr{E}}, w^{\mathscr{V}})$. Define $V(\theta) = L(\theta; w^{\mathscr{E}}, w^{\mathscr{V}}) - L(\theta^*; w^{\mathscr{E}}, w^{\mathscr{V}})$. It is trivial to see $V(\theta)$ is a Lyapunov function for the system. Moreover, $\dot{V}(\theta) = 0$ means $\dot{L}(\theta; w^{\mathscr{E}}, w^{\mathscr{V}}) = 0$. The only

scenario this can happen is at the equilibrium. As a result, the equilibrium $\theta^*(w^{\mathscr{E}}, w^{\mathscr{V}})$ is asymptotically stable. Proof complete. ■

Theorem IV basically states an event-triggered distributed algorithm. This theorem asserts that each generator i's phase angle $\theta_i(t)$ needs to follow the direction suggested by equation 23. When the inequality in equation 25 is violated, generator i will trigger the sampling and transmission of generator state φ_i to its neighboring generators. Generator i compares the error between the last transmitted state $\hat{\varphi}_i$ and the current state φ_i. At the sampling time $T_i[\ell]$, this difference is zero and the inequality is trivially satisfied. After that time, the difference increases and when the inequality in equation 25 is violated, we let that time be the next sampling instant, $T_i[\ell+1]$ and then transmit the sampled generator state $\hat{\varphi}_i$ to the neighboring generators $k \in \mathscr{N}_i$. The theorem asserts that if all the generators behave in the above way, then the generated power of all generators will approach the solution of the OPF problem.

It turns out that the above algorithm can be easily integrated into the CERTS microgrid controller. It is achieved by dynamically adjusting the requested power P_{req} for each generator. In the microsource controller in [13], generator i's phase angle θ_i is adjusted by comparing the measured active power P_{G_i} and the requested power $P_{req,i}$, where θ_i follows

$$\dot{\theta}_i(t) = \pi(P_{req,i} - P_{G_i}(t)) \tag{26}$$

This suggests that if instead of fixing $P_{req,i}$, which is what has been done in [13], we can adjust $P_{req,i}$ so that the direction suggested by equation 26 matches the direction suggested by our event-triggered scheme in equation 23. This can be easily done by setting

$$P_{req,i}(t) = P_{G_i}(t) - \frac{\gamma z_i(t)}{\pi} \tag{27}$$

Here $\gamma > 0$ is a constant that controls how fast we adjust the phase angle. This constant is necessary because if $z_i(t)$ is large, the adjustment in θ_i may be too fast, which as a result may destabilize the system. Since generator i can compute both P_{G_i} and z_i locally, $P_{req,i}$ can be easily computed by generator i itself. This suggests that each generator only needs to adjust its power set point according to equation 27. It samples and then broadcasts its state φ_i to its neighboring generators when the inequality in equation 25 is violated. If every generator follows this action, then by theorem IV, the generated power P_G of all generators will approach the solution of OPF.

V. SIMULATION

This section presents simulation results. The simulation is done in MATLAB/SimPower and shows that our algorithm indeed solves the OPF problem in a distributed way, and the communication between neighboring subsystems is very infrequent.

We use a three bus example based on a CERTS testbed at UWM, which is shown in figure 3. The network consists of three generators with power set point $0.4, 0.8, 0.6$ (pu) respectively. There are three active loads which request $0.96, 0.72, 0.48$ (pu) active power, respectively. Transmission lines are assumed to have zero resistance and all have impedances of $z = 0.0039\,j$. Each generator has generating limits between 0pu and 1pu. Each transmission line has power flow limits between -0.4pu to 0.4pu. The cost functions of the three generators are: $2.0+0.1p+0.1p^2$, $3.0+1.8p+0.1p^2$, $1.0+0.5p+0.1p^2$. All generators come online at $t = 0$s with their initial fixed power set points. At $t = 3$s, we switch from the fixed power set point scheme to our event-triggered set point scheme. At $t = 10$s, the third load is added to bus 2.

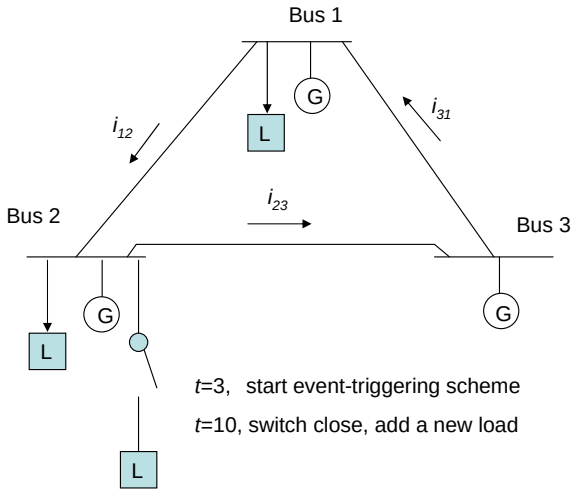

Fig. 3. Three generator simulation model

Figure 4 plots the generator power as a function of time. The left three plots correspond to generators' measured power, and the right three plots correspond to the set points computed by equation 27 for three generators. We can see that the actual measured power tracks the computed set point very well. After switching to the event-triggered scheme at $t = 3$s, generator 1 quickly increases its generation to full capacity, because it has the lowest generation cost. At the same

time, generator 2's generation drops to minimum, because it is the most expensive generator. When the new load is added at $t = 10$s, generator 1 cannot increase its generation further since it is already at full capacity, so generator 2 picks up the additional load. Figure 4 shows that our event-triggered scheme does adjust the power set point in a way that favors the low cost generator. Also the generating limit constraint is satisfied when using our new controller to adjust set point.

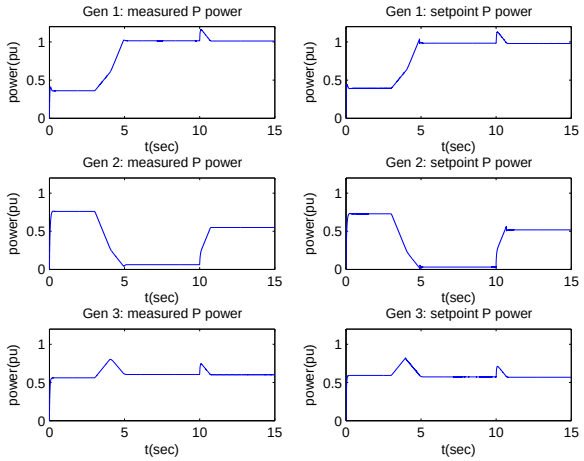

Fig. 4. Measured generator power and generator power set point

Figure 5 plots the power flow on the transmission line as a function of time for all three transmission lines. The important thing to notice here is that in the middle plot, the power flow on the transmission line is kept below 0.4pu, the flow limit of the line. At $t = 10$s, because of the addition of a load, the flow limit on the second transmission line is violated for less than 1s, but the power flow quickly adjusts back to within the limit. Both figure 4 and figure 5 show that our algorithm reacts very quickly to the changes in the network.

Figure 6 plots the broadcast periods of the generators as a function of time. The y-axis represents the time passed since the last broadcast. This figure shows some very interesting result. Both the second and the third generator have broadcasted only twice, and the first generator broadcasted 9 times. If we compare figure 6 with figure 4, we will find out that only the first generator's generating limit constraint is active. This explains why it triggers much more often. For generator 2 and 3, they only need to broadcast their states occasionally or when some

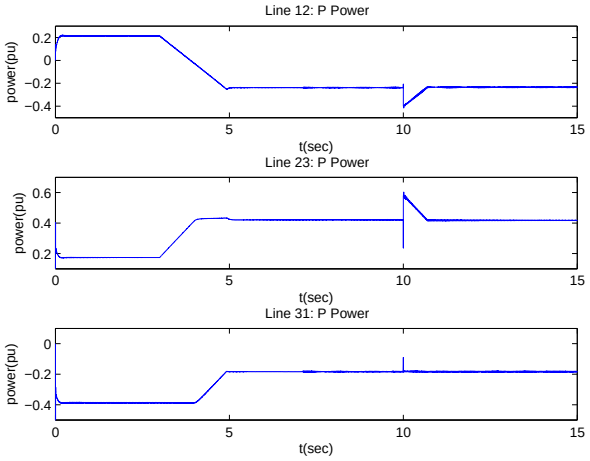

Fig. 5. Transmission line power flow

network condition changes. For generator 1, it has an active generating limit constraint, so it is more likely to broadcast its state. As we can see from the figure, most of the time the generators do not need to communicate with their neighbors at all (almost 5 secs for generator 2), this is highly desirable and has the potential to significantly reduce the communicate costs of a large scale power system.

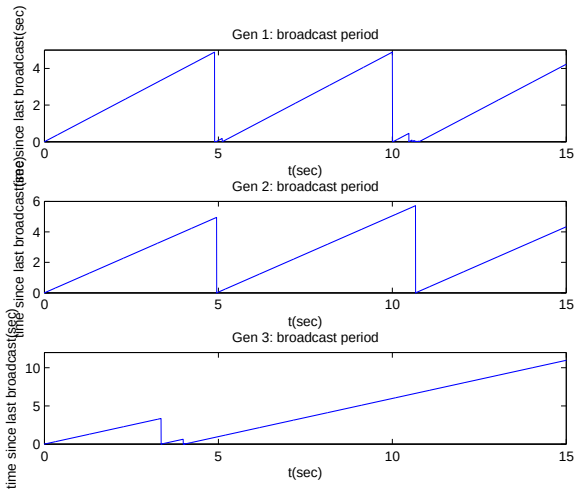

Fig. 6. Broadcast period of generators

Finally in figure 7 we plot the total generation cost as a function of time. Without any surprise,

our scheme reduces the initial generation cost of 7.8 when using fixed set point scheme to about 6.6. This is a reduction of about 15%, which is significant.

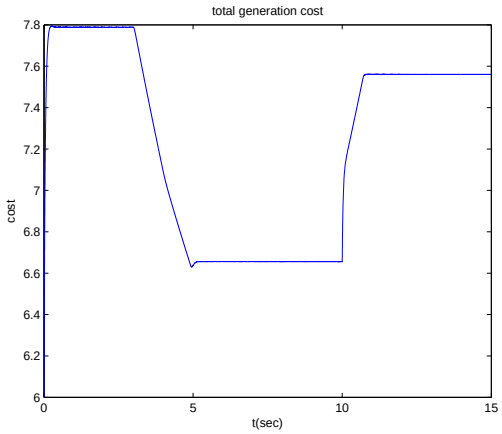

Fig. 7. Total generation cost

REFERENCES

[1] K. E. Arzen. A simple event based pid controller. In *Proc. 14th IFAC World Congress*, 1999.

[2] K.J. Astrom and B.M. Bernhardsson. Comparison of riemann and lebesgue sampling for first order stochastic systems. In *Proceedings of the IEEE Conference on Decision and Control*, volume 2, pages 2011–2016, 2002.

[3] D.P. Bertsekas. *Nonlinear programming*. Athena Scientific, 1999.

[4] PN Biskas, AG Bakirtzis, NI Macheras, and NK Pasialis. A decentralized implementation of DC optimal power flow on a network of computers. *IEEE Transactions on Power Systems*, 20(1):25–33, 2005.

[5] B. Bollobás. *Modern Graph Theory*. Springer, 1998.

[6] MF Carvalho, S. Soares, and T. Ohishi. Optimal active power dispatch by network flow approach. *IEEE Transactions on Power Systems*, 3(4):1640–1647, 1988.

[7] RD Christie, BF Wollenberg, and I. Wangensteen. Transmission management in the deregulated environment. *Proceedings of the IEEE*, 88(2):170–195, 2000.

[8] AJ Conejo and JA Aguado. Multi-area coordinated decentralized DC optimal power flow. *IEEE Transactions on Power Systems*, 13(4):1272–1278, 1998.

[9] AL Dimeas and ND Hatziargyriou. Operation of a Multiagent System for Microgrid Control. *Power Systems, IEEE Transactions on*, 20(3):1447–1455, 2005.

[10] S. Granville, E. CEPEL, P.R. Center, and R. de Janeiro. Optimal reactive dispatch through interior point methods. *Power Systems, IEEE Transactions on*, 9(1):136–146, 1994.

[11] CA Hernandez-Aramburo, TC Green, N. Mugniot, and I.C. London. Fuel consumption minimization of a microgrid. *Industry Applications, IEEE Transactions on*, 41(3):673–681, 2005.

[12] BH Kim and R. Baldick. A comparison of distributed optimal power flow algorithms. *IEEE Transactions on Power Systems*, 15(2):599–604, 2000.

[13] R. Lasseter. Control and design of microgrid components. Final Project Report - Power Systems Engineering Research Center (PSERC-06-03), 2006.

[14] R.H. Lasseter and P. Paigi. Microgrid: a conceptual solution. In *Power Electronics Specialists Conference, 2004. PESC 04. 2004 IEEE 35th Annual*, volume 6, pages 4285–4290 Vol.6, June 2004.

[15] L. Montestruque and M.D. Lemmon. Csonet: a metropolitan scale wireless sensor actuator network. In *Proceedings of the International Workshop on Mobile Device and Urban Sensing (MODUS)*, 2008.

[16] ARL Oliveira, S. Soares, and L. Nepomuceno. Optimal active power dispatch combining network flow and interior point approaches. *Power Systems, IEEE Transactions on*, 18(4):1235–1240, 2003.

[17] T. Ruggaber, J. Talley, and L. Montestruque. Using embedded sensor networks to monitor, control, and reduce CSO events: A pilot study. *Environmental Engineering Science*, 24(2):172–182, 2007.

[18] J. Sandee, W. Heemels, and P. van den Bosch. Case studies in event-driven control. In *Hybrid Systems: Computation and Control*, pages 762–765. Springer, 2007.

[19] Tabuada. Event-triggered real-time scheduling of stabilizing control tasks. *IEEE transactions on automatic control*, 52(9):1680, 2007.

[20] Y.Z. Tsypkin. *Relay Control Systems*. Cambridge University Press, 1984.

[21] P. Wan and M. D. Lemmon. Distributed Network Utility Maximization using Event-triggered augmented Lagrangian methods. In *Proceedings of American Control Conference*, 2009.

[22] X. Wang and M. Lemmon. Self-triggered feedback control systems with finite-gain l 2 stability. *IEEE transactions on automatic control*, 54:452, 2009.

[23] X. Wang and M.D. Lemmon. Event-triggering in distributed networked systems with data dropouts and delays. In *Proceedings of Hybrid Systems: computation and control*, 2009.